*Meteoritics & Planetary Science* 37, 1843–1856 (2002)
Available online at http://www.uark.edu/meteor

# Dark inclusions in the Mokoia CV3 chondrite: Evidence for aqueous alteration and subsequent thermal and shock metamorphism

ICHIRO OHNISHI AND KAZUSHIGE TOMEOKA*

Department of Earth and Planetary Sciences, Faculty of Science, Kobe University, Nada, Kobe 657-8501, Japan
*Correspondence author's e-mail address: tomeoka@kobe-u.ac.jp

*(Received 2002 April 22; accepted in revised form 2002 August 27)*

**Abstract**–Mokoia is a CV3 chondrite that contains abundant phyllosilicate mineralization. We present a detailed petrographic and scanning electron microscopic study of 24 dark inclusions (DIs) that we found in Mokoia. The overall texture and constituent minerals of the DIs resemble those in the host meteorite. Fe-bearing saponite and Na-rich phlogopite, the same phyllosilicates as in the host meteorite, occur in the DIs, which strongly suggests that the DIs have a similar alteration history to the host meteorite. However, the DIs show several distinct differences from the host meteorite. Olivine grains in the DI matrices are more homogeneous in Fe/(Fe + Mg) ratio than those in the host meteorite matrix. Phyllosilicates in the DIs are less abundant than in the host meteorite, and they have been dehydrated to various extents. These characteristics suggest that the DIs have experienced higher degree of thermal metamorphism than the host meteorite. In addition, the matrices in the DIs are more compacted than those in the host meteorite. Most olivine grains in the DIs show undulatory extinction in transmitted crossed-polarized light and some show planar fractures, while such olivine grains are rare in the host meteorite. Two of the DIs contain Si-, Mg-, Fe- and O-rich melt veins. These characteristics indicate that most DIs have been shocked to shock stage S3–S4, while the host meteorite is shock stage S1 (virtually unshocked). Thermal metamorphism of the DIs was likely caused by shock heating. These results are consistent with the contention previously proposed for the DIs in CV3 chondrites (*i.e.*, the DIs have experienced aqueous alteration and subsequent dehydration on the CV parent body). We suggest that thermal and shock metamorphism occurred locally to various extents after pervasive aqueous alteration in the Mokoia parent body.

## INTRODUCTION

Dark inclusions (DIs) are common in CV3 chondrites, and most previous work on DIs has been done from this type of chondrites (Fruland *et al.*, 1978; Johnson *et al.*, 1990). However, a recent study (Itoh and Tomeoka, 2002) revealed that DIs are also common in CO3 chondrites, although DIs in CO3 chondrites are smaller in size than those in CV3 chondrites. So DIs are apparently more important constituents of these type-3 chondrites than previously thought. DIs in CV3 chondrites are lithic clasts that range in size from 1 mm to a few centimeters. Based on texture, they can be mainly divided into three types; A, B and C (Krot *et al.*, 1995). Type A and B constitute two endmembers in a range of continuous variations in texture; type A contains chondrules in a fine-grained matrix and so is similar to the host chondrites, whereas type B consists entirely of fine grains of Fe-rich olivine, lacks chondrules, and instead contains rounded porous aggregates of Fe-rich olivine. Some workers suggested that the rounded porous aggregates were pseudomorphs of chondrules (Kojima *et al.*, 1993; Kojima and Tomeoka, 1996; Krot *et al.*, 1997). Type C consists mostly of fine grains of Fe-rich olivine and are devoid of chondrules and porous aggregates. Despite these textural variations, DIs are similar in bulk chemical, oxygen-isotopic and noble gas-isotopic composition to their host CV3 chondrites (Palme *et al.*, 1989; Johnson *et al.*, 1990; Bunch *et al.*, 1980).

The origin of DIs in CV3 chondrites has been the subject of controversy for the last decade; opinions have been mainly divided into the following two categories: DIs are (1) primary aggregates of condensates from the solar nebula (Kurat *et al.*, 1989; Palme *et al.*, 1989), or (2) fragments of a CV-like parent body that were aqueously altered and subsequently dehydrated on the parent body (Kojima *et al.*, 1993; Kojima and Tomeoka, 1996; Buchanan *et al.*, 1997; Krot *et al.*, 1997, 1998a,b, 1999). Recent studies on DIs in CV3 chondrites have presented much evidence for parent-body processes (model (2)) (*e.g.*, a network of fracture-filling veins, pseudomorphs of chondrules and calcium-aluminum-rich inclusions (CAIs), fibrous olivines similar to dehydrated phyllosilicates, *etc.*). However, there still remain opinions against this model. A major problem raised against this model is the lack of hydrous minerals, such as phyllosilicates, that are characteristic of the hydration process



Prelude preprint MS#4820

(*e.g.*, Kurat *et al.*, 1989; Johnson *et al.*, 1990; Weisberg and Prinz, 1998). Most of the DIs reported from CV3 chondrites consist, like host chondrites, almost entirely of anhydrous minerals. The lack of hydrous minerals also hinders our understanding of the proposed dehydration process: it has been argued that if the dehydration process occurred to minor degrees, as required to maintain the unrecrystallized, porous texture of DI matrices, one would expect to find relics of the hydration process. Some workers also argued that if DIs were heated to high temperatures to dehydrate phyllosilicates, there should remain other independent evidence of such temperatures such as the initiation of olivine equilibration (*e.g.*, Weisberg and Prinz, 1998).

Mokoia is an unusual member of the CV3 group that contains abundant phyllosilicates in a matrix, chondrules and CAIs (Cohen *et al.*, 1983). Using a transmission electron microscope (TEM), Tomeoka and Buseck (1990) showed evidence that phyllosilicates in Mokoia have been produced by aqueous alteration of anhydrous silicates probably on the meteorite parent body. In addition, matrix olivines in Mokoia are especially highly unequilibrated among the known CV3 chondrites (Scott *et al.*, 1988), which indicates that this meteorite has not experienced any significant degree of thermal metamorphism. Therefore, we thought that DIs in Mokoia, if any were found, would be the best target to address the problems raised against the parent-body origin for DIs (model (2)). Cohen *et al.* (1983) found a DI from Mokoia, but provided no mineralogical and petrographic details. Through the courtesy of Dr. J. A. Wood, we were granted an opportunity to examine a total of six Mokoia thin sections, including the five thin sections that Cohen *et al.* studied. We have performed an extensive, detailed survey of those thin sections using a scanning electron microscope (SEM), and have found a total of four large (>0.8 mm in size) DIs, one of which is the same as the one that Cohen *et al.* described, as well as many smaller DIs. We here present the results of a detailed mineralogical and petrographic study of those DIs. Our goals are to clarify the genetic relationship between the DIs and their host meteorite, and to determine whether or not the DIs have experienced an aqueous alteration and subsequent dehydration process as proposed for the origin of DIs in other CV3 chondrites.

## MATERIALS AND METHODS

Six polished thin sections of Mokoia (271.6 $mm^2$ total area) were studied using an optical microscope, a SEM (JEOL JSM-5800) equipped with an energy dispersive x-ray spectrometer (EDS), and an electron probe microanalyzer (EPMA) (JEOL JXA-8900) equipped with wavelength dispersive x-ray spectrometers (WDS). EDS analyses were obtained at 15 kV and 0.4 nA, and WDS analyses at 15 kV and 12 nA. Data corrections were made by the Phi-Rho-Z method for the EDS analysis and by the Bence–Albee method for the WDS analysis. Well-characterized natural and synthetic minerals and glasses were used as standards. For the analysis of each mineral grain, we used a focused electron beam of ~2 $\mu$m in diameter. For the analysis of fine-grained matrices, we used a defocused electron beam of 10–50 $\mu$m in diameter. X-ray chemical mapping analysis was performed by using the EPMA. We note that the petrographic thin sections that we studied were not prepared for a demounting purpose, so it was not possible to do a TEM observation of them.

Porosity measurements of fine-grained matrices of DIs 1–4 and the host meteorite were performed by using an image processing method similar to what Corrigan *et al.* (1997) and Nakamura *et al.* (2000) used. Digitized high-resolution backscattered electron (BSE) images were obtained of five different randomly selected areas, each of which is $40 \times 30$ $\mu m^2$ in area, in each matrix of the DIs and the host meteorite. Each of those images was converted, using the Adobe Photoshop software package, to a histogram showing a brightness distribution of individual pixels in the image. After determining a proper threshold level in the histogram, a 255 level black and white image was converted to a straight black/white (0/255) image. A porosity of the selected area was calculated as an area percentage of black spaces (which correspond to void spaces in matrix) to a whole image.

## PETROGRAPHY AND MINERALOGY

### General Petrography

A total of four unusual inclusions that are brownish to greyish in transmitted plane-polarized light have been found in three of the six thin sections of Mokoia that we studied. Those dark inclusions (named DI-1 to 4) are angular to irregular in shape and range in size from $1.4 \times 0.8$ to $2.3 \times 1.7$ mm (Table 1; Fig. 1). All the DIs contain chondrules, chondrule fragments and fragments of a variety of minerals in fine-grained matrices. In BSE images, matrices of the DIs show distinctly brighter contrast than the matrix of the host meteorite (Fig. 1), which suggests that the former have a higher atomic number density than the latter. In addition to those four DIs, a total of 20 smaller inclusions (50–1000 $\mu$m in size) that are similar in mineralogy and texture to DIs 1–4 have been found in the thin

TABLE 1. Sizes of dark inclusions and porosities of matrices in dark inclusions and the host Mokoia meteorite.

| | Size (mm) | Porosity of matrix (%) |
|---|---|---|
| Dark inclusions | | |
| DI-1 | $2.7 \times 1.2$ | 1.5–5.4 |
| DI-2 | $1.4 \times 0.8$ | 4.7–8.1 |
| DI-3 | $1.8 \times 1.2$ | 0.2–1.8 |
| DI-4 | $2.3 \times 1.7$ | 0.2–2.1 |
| Host meteorite | – | 15.3–27.9 |

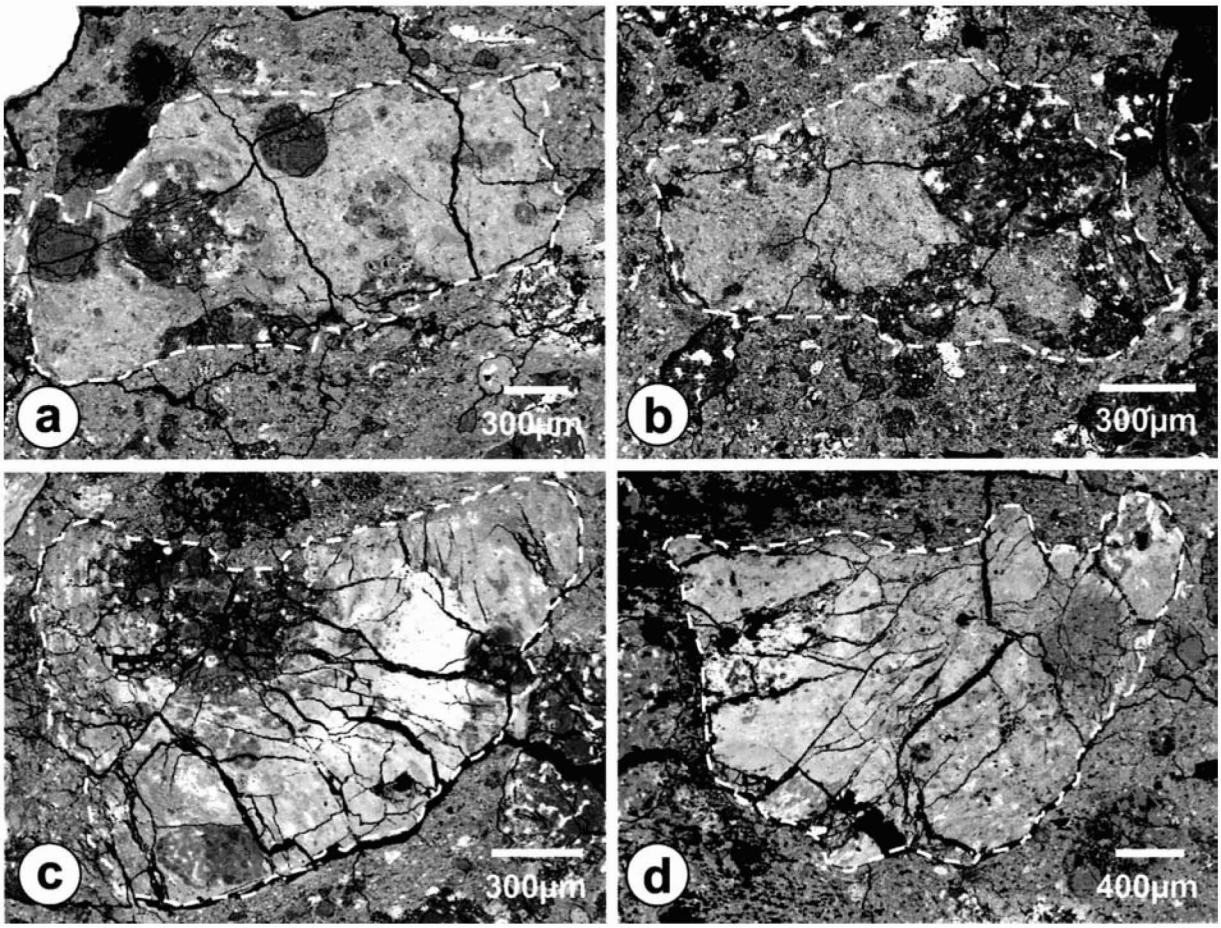


FIG. 1. Backscattered electron images of dark inclusions (DIs; outlined by white broken lines) in the Mokoia CV3 chondrite. (a) DI-1. (b) DI-2. (c) DI-3. (d) DI-4. The DIs are distinctly brighter relative to the host meteorite. DI-3 and DI-4 have high densities of fractures; most of them terminate at the boundary between the DIs and the host meteorite.

sections. In the following descriptions we treat these small inclusions similarly as DIs but mainly focus on DIs 1–4. DI-1 is the same as what Cohen *et al.* (1983) described as a "dark clast" (Fig. 1b in their paper). The total area of all the 24 DIs in the six thin sections is 9.5 $mm^2$ (3.5 vol%).

DI-3 and DI-4, in particular, have high densities of fractures that range in width from 2 to 30 $\mu$m and in length from 100 to 1000 $\mu$m (Figs. 1c,d and 8a). The fractures penetrate matrix and chondrules and form a network throughout each DI. Fractures are not random in direction; they occur, in some areas, roughly in parallel orientation (see Fig. 8a). Such high densities of fractures are not observed in any areas of the host meteorite. Most of the fractures terminate at the boundaries between the DIs and the host meteorite, which suggests that the fractures formed before or during incorporation of the DIs to the present location. Most coarse grains of olivine (>50 $\mu$m in size) in DI-3 and DI-4 exhibit undulatory extinction in transmitted crossed-polarized light. Six out of 17 (~35%) coarse grains of olivine show planar fractures. From these properties of olivine, DI-3 and DI-4 can be assigned to shock stage S3 or higher. Planar fractures were not observed in olivines in other DIs, and rare in the host Mokoia meteorite that is assigned to shock stage S1 (virtually unshocked) (Scott *et al.*, 1992).

## Chondrules and Other Coarse-Grained Components

A total of 43 chondrules and chondrule fragments (100–800 $\mu$m in diameter) have been found in the DIs. They have porphyritic olivine (~84%), porphyritic olivine-pyroxene (~14%) and barred olivine (~2%) textures. In addition, three amoeboid olivine aggregates (AOAs; 130–410 $\mu$m in diameter) and one CAI (~270 $\mu$m) have been found. The CAI contains concentric nodules (5–20 $\mu$m in diameter), each having a spinel core surrounded by phyllosilicate and diopside rims. These chondrules, AOAs and CAI are almost indistinguishable from those typical in the host meteorite. A notable characteristic uncommon in the host meteorite is that most opaque nodules, which consist largely of magnetite and pentlandite, in

chondrules, especially those occurring near margins of chondrules, have large Fe-rich halos (Fig. 2b,d); this suggests that Fe diffused out from the Fe-rich opaque minerals.

All the chondrules, AOAs and CAI in the DIs contain various amounts of phyllosilicates. In the chondrules and AOAs, phyllosilicates replace mesostases and enstatite (Fig. 2c), and less commonly Fe-rich olivine. In the CAI, phyllosilicates replace most constitutent minerals except spinel and diopside. Microprobe analyses show that phyllosilicates replacing enstatite and olivine are Fe-bearing saponite, whereas those replacing chondrule mesostases and the CAI are intergrowths of Na-rich phlogopite and serpentine (Table 2). Fe-bearing saponite and Na-rich phlogopite-serpentine intergrowths commonly occur in intimate mixtures. The occurrence, texture and mineral species of phyllosilicates are identical to those in the host meteorite. The major element abundances of phyllosilicates in the DIs also resemble those in the host meteorite (Fig. 3) except that Fe tends to be slightly more enriched in the DI phyllosilicates (Table 2). However, phyllosilicates in the DIs show distinctly higher analytical totals (76.7–96.3 wt%, 87.1 wt% in average) than those in the host meteorite (61.8–92.4 wt%, 80.5 wt% in average). Saponite in the DIs and the host meteorite especially shows more distinctive differences in analytical total (86.3 *vs.* 76.1 in average) than other phyllosilicates (Fig. 4). Analytical totals of phyllosilicates within a DI are similar to each other, but differ considerably among DIs; there is an apparent tendency that analytical totals of phyllosilicates in DI-3 and DI-4 are higher than those in DI-1 and DI-2 (90.9 *vs.* 85.8 wt% in average).

## Matrices and Chondrule Rims

The matrices of the DIs consist mainly of fine grains (5–30 $\mu$m in size) of Fe-rich olivine that occur in platy, lath-shaped to blocky morphologies (Fig. 5). Minor minerals in matrix include, roughly in decreasing order, magnetite, Fe-Ni sulfides

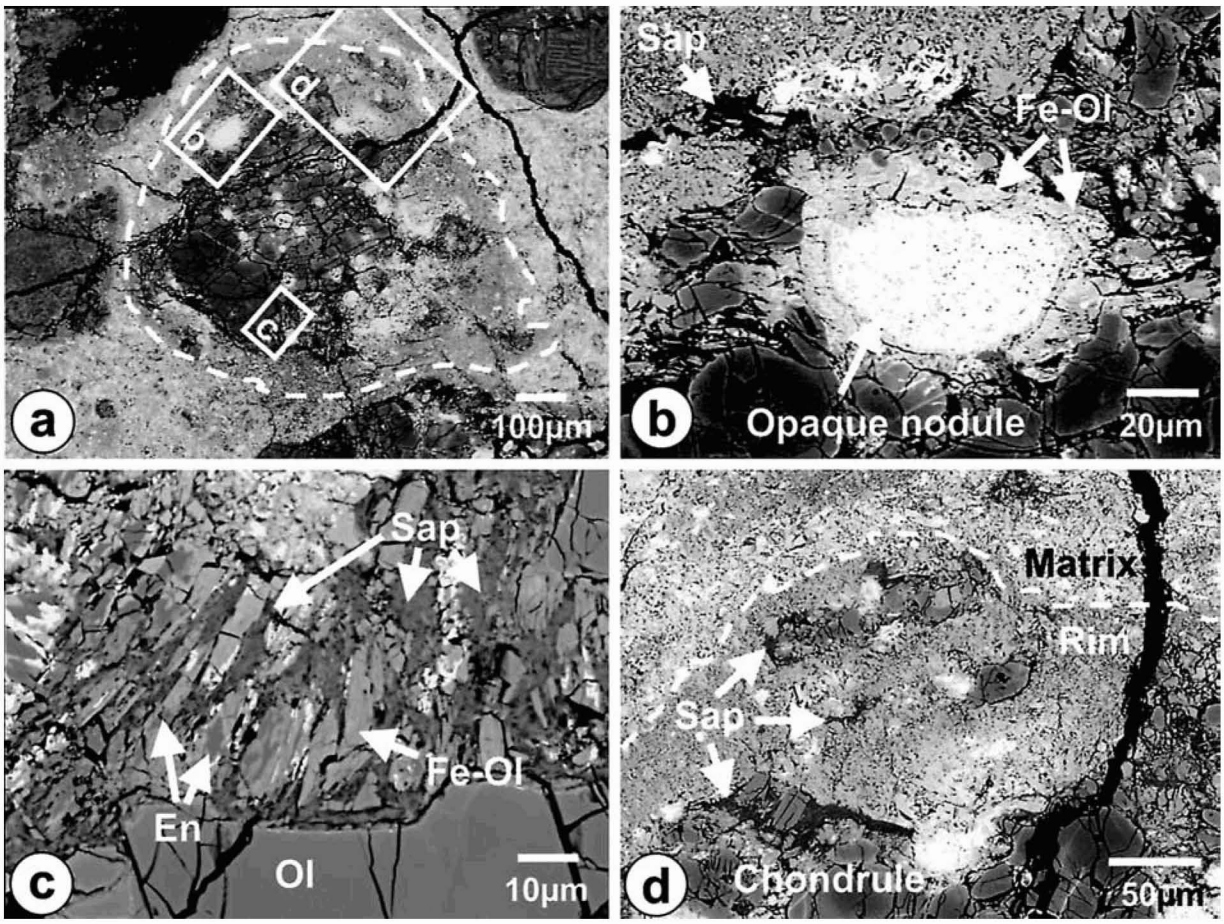


FIG. 2. (a) Backscattered electron image of a chondrule in DI-1. Outlined by a white broken line is a fine-grained rim that surrounds the chondrule. (b) Image of boxed area (b) in (a), showing a bright Fe-rich halo (Fe-rich olivine (Fe-Ol)) of an opaque nodule (magnetite and pentlandite) located near the chondrule edge. (c) Image of boxed area (c) in (a), showing a portion of the chondrule margin, in which saponite (Sap) forms by replacing enstatite (En) and Fe-rich olivine. (d) Image of boxed area (d) in (a), showing a portion of the boundary between the chondrule and the rim. A bright Fe-rich halo of an opaque nodule (magnetite and pentlandite) located near the chondrule edge extends widely into the fine-grained rim.

TABLE 2. Selected electron microprobe analyses of phyllosilicates in chondrules in the host Mokoia meteorite and dark inclusions (wt%).

| | Mokoia host | | | | | | Dark inclusions | | | | |
|---|---|---|---|---|---|---|---|---|---|---|---|
| | Saponite | | | | Phl–Srp | | Saponite | | | | Phl–Srp |
| | 1 | 2 | 3 | 4 | 5 | 6* | 1† | 2† | 3‡ | 4‡ | 5† |
| $SiO_2$ | 44.7 | 46.2 | 42.1 | 45.1 | 34.7 | 36.4 | 45.7 | 45.5 | 51.2 | 50.8 | 35.3 |
| $TiO_2$ | 0.18 | 0.43 | 0.13 | 0.20 | 0.08 | 0.32 | 0.11 | 0.11 | 0.15 | 0.13 | 0.06 |
| $Al_2O_3$ | 4.53 | 5.13 | 4.88 | 6.38 | 20.2 | 20.8 | 8.33 | 8.02 | 7.06 | 8.29 | 21.7 |
| $Cr_2O_3$ | 0.97 | 1.50 | 0.31 | 0.48 | 0.04 | 0.02 | 1.49 | 1.63 | 1.46 | 1.17 | 0.09 |
| FeO | 2.07 | 2.20 | 3.05 | 3.00 | 3.40 | 3.73 | 4.20 | 5.20 | 6.24 | 4.61 | 4.98 |
| MnO | n.d. | 0.01 | 0.01 | 0.04 | 0.04 | 0.07 | n.d. | n.d. | n.d. | 0.01 | 0.04 |
| MgO | 23.2 | 24.4 | 22.1 | 23.7 | 21.4 | 19.7 | 24.2 | 24.5 | 24.6 | 25.7 | 23.4 |
| CaO | 0.15 | 0.15 | 0.10 | 0.11 | 0.58 | 1.24 | 0.38 | 0.37 | 0.21 | 0.17 | 0.70 |
| $Na_2O$ | 1.24 | 1.34 | 1.61 | 1.57 | 3.73 | 2.12 | 1.77 | 2.15 | 1.74 | 2.03 | 2.43 |
| $K_2O$ | 0.64 | 0.93 | 0.25 | 0.82 | 2.43 | 0.84 | 1.56 | 1.12 | 1.75 | 2.33 | 1.62 |
| Total | 77.7 | 82.4 | 74.6 | 81.4 | 86.6 | 85.2 | 87.7 | 88.6 | 94.5 | 95.2 | 90.3 |

*Obtained from a CAI.
†Obtained from DI-1.
‡Obtained from DI-3.
Abbreviations: n.d. = not detected; Phl–Srp = intergrowth of Na-rich phlogopite and serpentine.

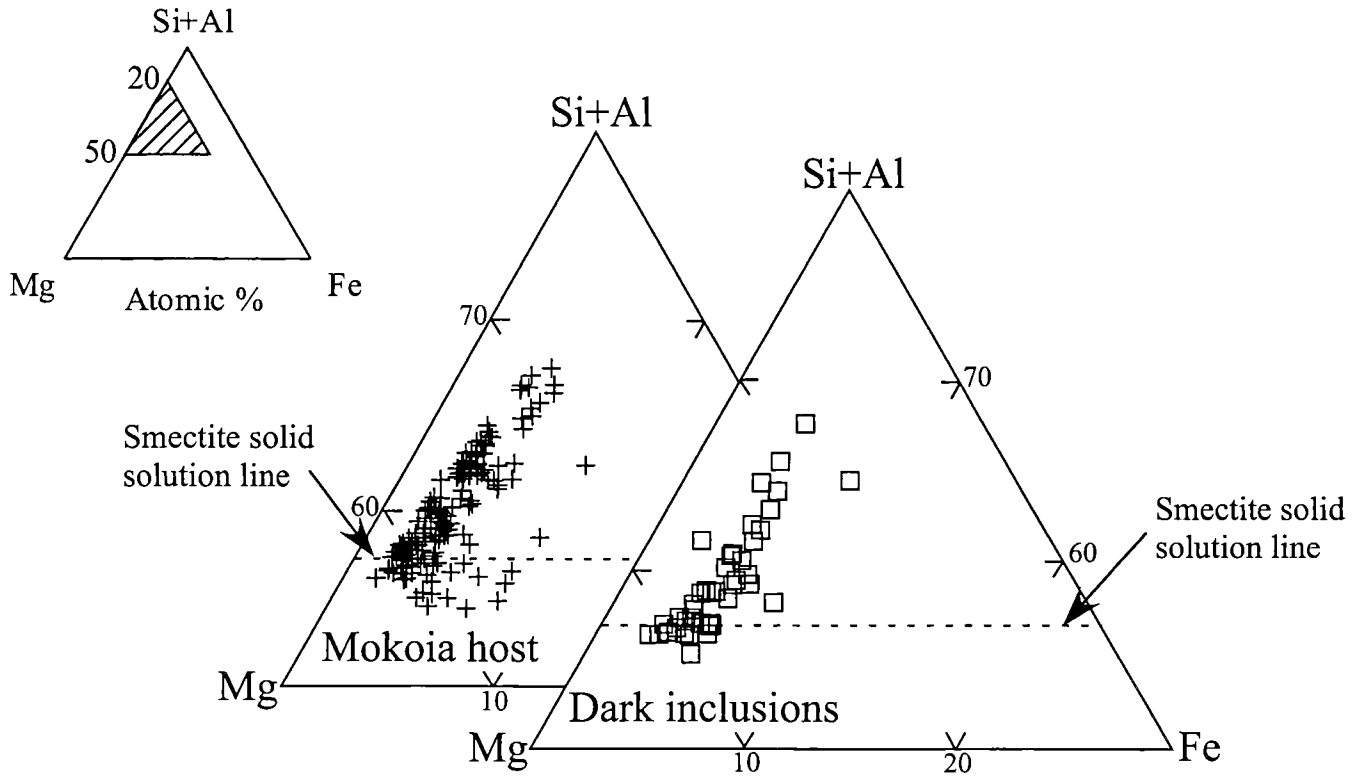


FIG. 3. Analyses of phyllosilicates in dark inclusions and Mokoia host in terms of atomic percents of Si + Al, Mg and Fe. Also shown are the ideal Mg-Fe solid solution lines of trioctahedral smectite ($(Mg, Fe)_3(Si, Al)_4O_{10}(OH)_2$).

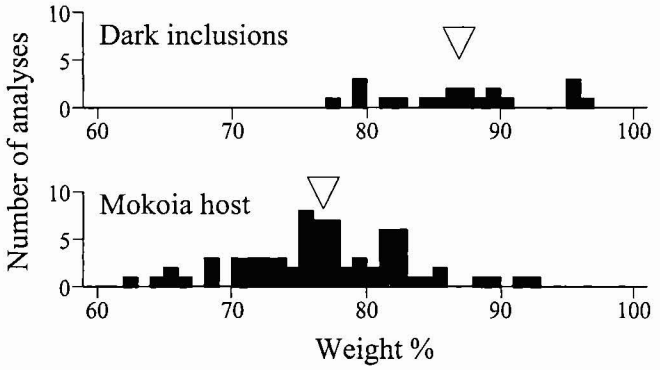


FIG. 4. Analytical totals of saponites in dark inclusions and Mokoia host. Indicated by open triangles are averages.

(pentlandite and minor Fe sulfide), Ca-Fe-rich clinopyroxenes, andradite, sodalite and phyllosilicates. In places, magnetite occurs as framboidal aggregates. Ca-Fe-rich clinopyroxenes and andradite commonly form intermixed aggregates (10–50 $\mu$m in diameter) that are commonly rounded in shape. The olivine morphologies and the occurrences of all the minor minerals are common with those in the host meteorite matrix. However, the DI matrices show mainly two distinct differences from the host meteorite matrix. First, olivine grains in the DI matrices are more homogeneous ($Fa_{45-65}$) in fayalite content and more Fe-rich, on the average, than those in the host meteorite matrix ($Fa_{2-99}$) (Fig. 6). Second, grains in the DI matrices are more compacted than those in the host meteorite matrix (Fig. 5). The measured porosities of the matrices of DIs 1–4 range from 0.2 to 8.1, whereas those of the host meteorite matrix range from 15.3 to 27.9% (Table 1). The Fe enrichment of olivine and the denser packing of the grains are apparently the main causes of the bright contrast of the DIs when imaged using BSE.

Compared to the matrices of DI-1 and DI-2, those of DI-3 and DI-4 are more highly compacted with the porosities of 0.2–2.1% (see Table 1). In highly compacted areas (<1.0% porosity), individual olivine grains are barely distinguishable in BSE images (Fig. 5c). In some areas, aggregates of magnetite and Fe-Ni sulfides and those of Ca-Fe-rich clinopyroxene and andradite are elongated along the same direction, exhibiting apparent foliation (Fig. 7). In those areas, fractures occur roughly in parallel to the direction of elongation; we note that the same feature has been observed in the experimentally shocked Murchison and Allende (Tomeoka *et al.*, 1999; Kiriyama *et al.*, 2000). Both DI-3 and DI-4 contain highly Fe-enriched areas (500 × 300 $\mu$m in DI-3 and 400 × 300 $\mu$m in DI-4) that exhibit very bright contrast in BSE images (Figs. 1c,d and 8); those areas contain coarse-grained aggregates (50–100 $\mu$m in size) of magnetite and pentlandite embedded in a fine-grained mixture of very Fe-rich olivine ($Fa_{70-90}$), pentlandite and magnetite (Fig. 8b). The Fe-rich olivine grains commonly contain minute inclusions (<0.2 $\mu$m in diameter) of magnetite

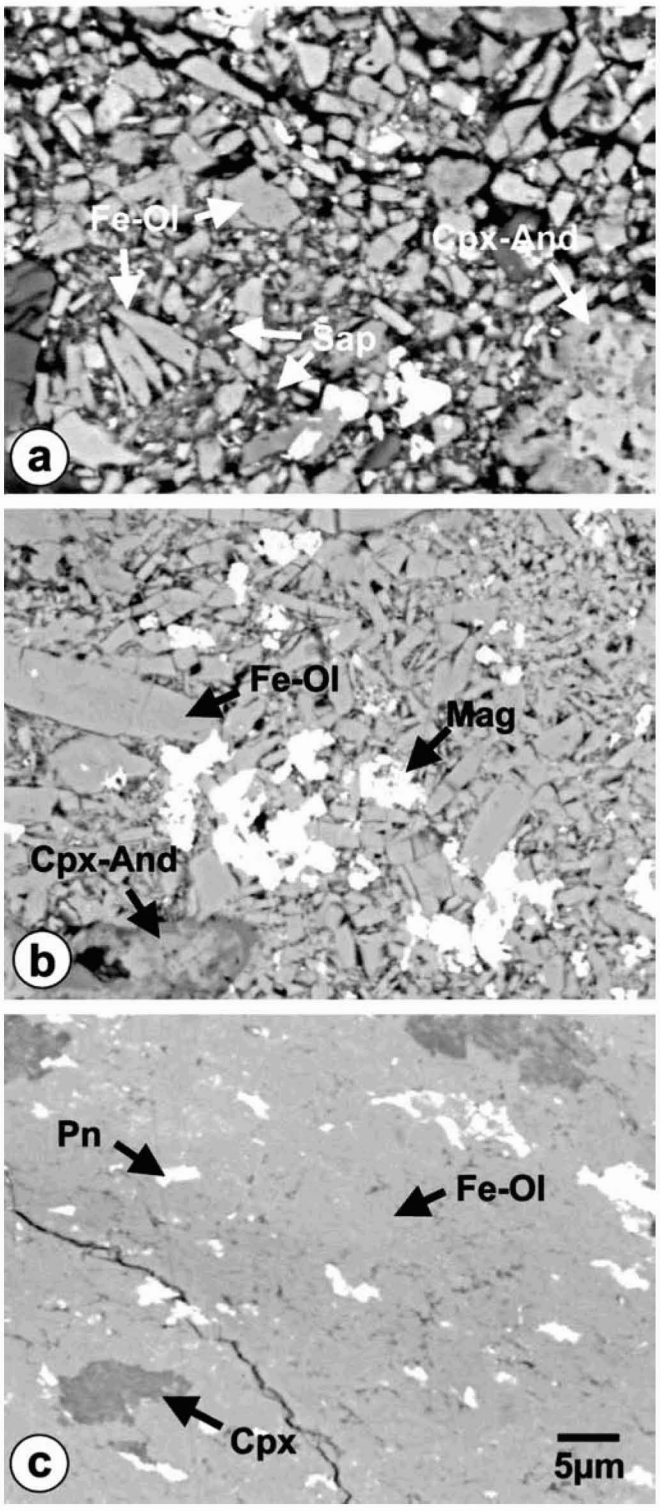


FIG. 5. Backscattered electron images of matrices in Mokoia host (a), DI-1 (b), and DI-3 (c). All the images are at the same magnification. Fe-Ol = Fe-rich olivine. Sap = saponite. Cpx = Ca-Fe-rich clinopyroxene. And = andradite. Mag = magnetite. Pn = pentlandite.

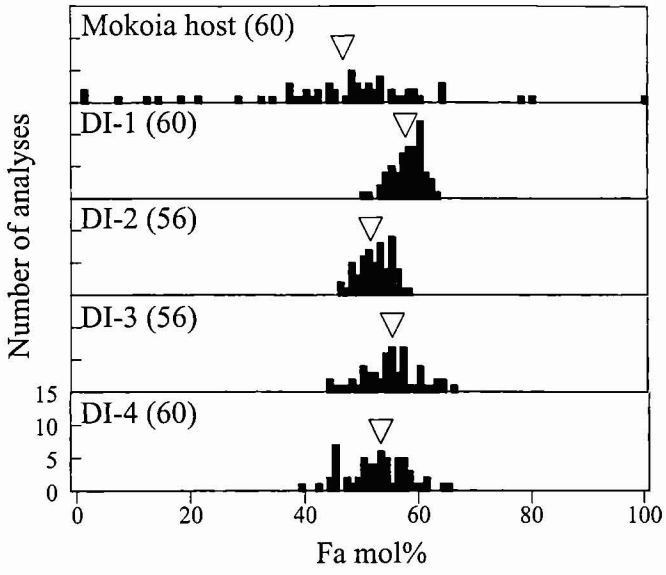


FIG. 6. Fayalite concentrations in matrix olivines in Mokoia host and dark inclusions. Indicated by open triangles are averages. Shown in the parentheses are number of analyses.

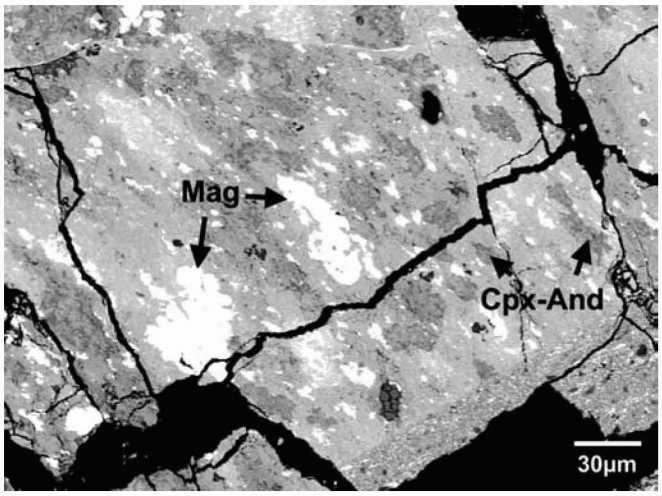


FIG. 7. Backscattered electron image of a portion of matrix in DI-3. Aggregates of magnetite (Mag) and those of Ca-Fe-rich clinopyroxene (Cpx) and andradite (And) are elongated along a northwest–southeast direction, exhibiting foliation.

and pentlandite. The abundance of Fe gradually decreases outward from the center of those areas, which suggests that Fe diffused out from those areas.

The matrices of all the 24 DIs contain variable amounts of Fe-bearing saponite that has compositions identical to those in chondrules in the DIs. Saponite occurs in interstices between olivine grains and in discrete clusters (10–40 $\mu$m in diameter); these occurrences are common with those in the host meteorite matrix. However, the abundance of saponite in the DI matrices is much lower than in the host meteorite matrix (Fig. 5). In most

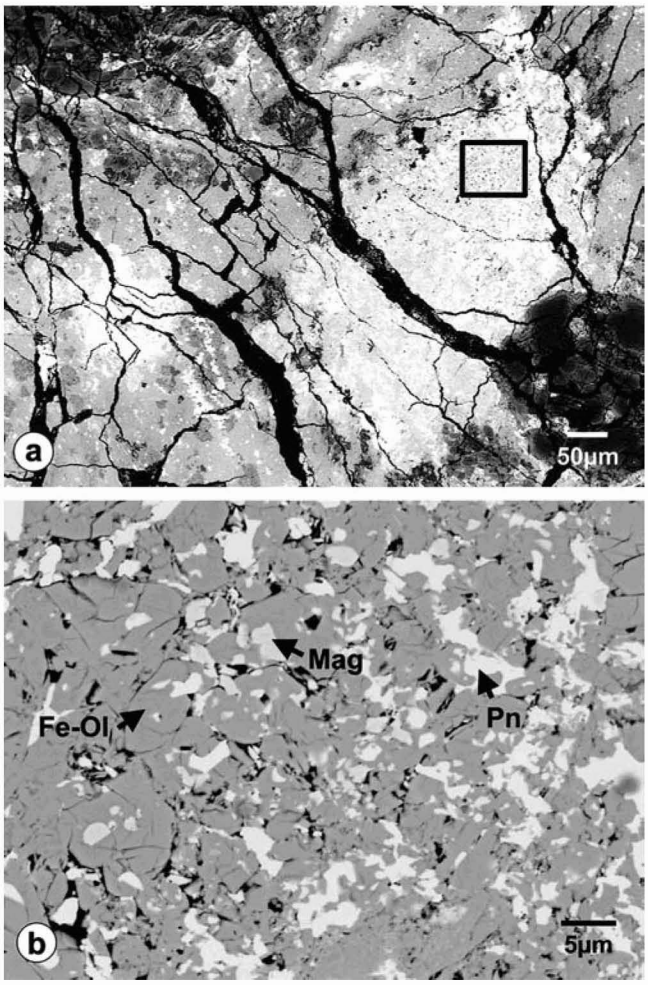


FIG. 8. (a) Backscattered electron image of a portion of DI-3 including very Fe-rich areas (bright) in matrix. (b) Low-contrast image of boxed area in (a), showing intermixed grains of Fe-rich olivine (Fe-Ol), magnetite (Mag) and pentlandite (Pn).

highly compacted areas, no saponite is detected by the microprobe analysis (Fig. 5c). The matrices in DI-3 and DI-4 contain lesser amounts of saponite than those in DI-1 and DI-2.

Approximately 33% of the chondrules and chondrule fragments, three AOAs and one CAI in the DIs are partly or entirely enclosed by fine-grained rims (*e.g.*, Fig. 2a,d). The rims consist of fine grains of minerals that are common with the matrices of the DIs. However, the rims tend to contain more magnesian olivine and higher amounts of saponite than the matrices, so appear darker in BSE images than the matrices. Such rims are also common in chondrules, AOAs and CAIs in the host meteorite. However, the differences in olivine composition and saponite abundance between rims and matrix are clearly smaller in the DIs than in the host meteorite; so in BSE images, boundaries between rims and surrounding matrices in the DIs are blurred and less distinctive than those in the host meteorite.

### Chemical Compositions of Matrices of Dark Inclusions

In order to examine bulk major element compositions of the matrices of DIs 1–4 and the host meteorite, we performed WDS analyses using a defocused beam. A major purpose of the analysis is to examine relationships between bulk compositions and the results of our mineralogical and petrographic observations. The analyses are shown in Table 3 and are also plotted in a (Si + Al)–Mg–Fe ternary diagram (Fig. 9). The matrices of the DIs are closely similar to each other, although analytical totals of the matrices of DI-3 and DI-4 are higher than those of DI-1 and DI-2. The matrices of the DIs and the host meteorite are also generally similar. However, there are significant differences as follows. First, analytical totals of the DI matrices are distinctly higher than that of the host meteorite matrix (89.2–95.6 *vs.* 80.9 wt%). This is consistent with the lower porosity and the lower abundance of phyllosilicates in the DI matrices relative to the host meteorite matrix. Second, the DI matrices are consistently higher in Fe/(Fe + Mg) ratio than the host meteorite matrix. This corresponds to the relatively high Fe contents of olivine grains in the DI matrices (cf., Fig. 6). Third, in the (Si + Al)–Mg–Fe ternary diagram (Fig. 9), the analyses of the DI matrices plot tightly on the olivine solid-solution line, whereas the analyses of the host meteorite matrix plot on an area that is distinctly off the olivine solid-solution line and on a line joining A (Fe/(Fe + Mg) = 0.07 on the smectite solid-solution line) and B (Fe/(Fe + Mg) = 0.54 on the olivine solid solution line). These are explained by that the DI matrices consist predominantly of olivine, whereas the host meteorite matrix consists mainly of olivine with composition B and minor amounts of saponite with composition A. Therefore, the bulk compositions of the matrices of the DIs and the host meteorite are generally consistent with the results of our mineralogical and petrographic observations.

### Melt Veins

An unusual material has been found in DI-3, which occurs as a gently curved, narrow band (10–70 $\mu$m in width and ~1000 $\mu$m in length) along an edge of the DI (Fig. 10). This material consists of dense aggregates of submicron-size granular grains that are rich in O, Si, Mg, Fe and Al (Table 3), and contains numerous rounded inclusions (1–2 $\mu$m in diameter) of pentlandite and magnetite and rounded pores (<1 $\mu$m) as well as angular to irregularly shaped fragments (1–10 $\mu$m) of forsterite, enstatite, Ca-rich clinopyroxene, plagioclase and spinel (Fig. 10d,e). From the texture, we inferred this material to be a melt. An identical material has also been found as a band (5–40 $\mu$m in width and 200 $\mu$m in length) in one of the small DIs (170 × 140 $\mu$m in size). In a portion of the banded material in DI-3 (see Fig. 10c,d), a small lenticular area (0–20 $\mu$m in width and 100 $\mu$m in length, indicated by a white arrow in Fig. 10c) that has the same lithology as the DI matrix occurs along the outside wall of the banded material; thus, in this portion, the banded material is sandwiched between the DI matrices. This texture suggests that the banded material occurred originally as a vein before separation of this DI from a parent material; most material on the side facing the host

TABLE 3. WDS defocused beam analyses of matrices in the host Mokoia meteorite, dark inclusions and a melt vein in DI-3 (wt%).

| | Mokoia host | | DI-1 | | DI-2 | | DI-3 | | DI-4 | | Melt vein* | |
|---|---|---|---|---|---|---|---|---|---|---|---|---|
| *N* | 111 | (s.d.) | 10 | (s.d.) | 10 | (s.d.) | 10 | (s.d.) | 10 | (s.d.) | 20 | (s.d.) |
| $SiO_2$ | 25.2 | (1.5) | 26.0 | (1.2) | 27.2 | (1.0) | 29.1 | (1.1) | 29.1 | (1.4) | 30.6 | (1.0) |
| $TiO_2$ | 0.06 | (0.03) | 0.08 | (0.06) | 0.03 | (0.01) | 0.03 | (0.03) | 0.03 | (0.01) | 0.10 | (0.02) |
| $Al_2O_3$ | 3.09 | (0.64) | 1.34 | (0.51) | 2.12 | (0.43) | 1.30 | (0.21) | 1.72 | (0.19) | 1.06 | (0.12) |
| $Cr_2O_3$ | 0.36 | (0.07) | 0.30 | (0.10) | 0.30 | (0.07) | 0.31 | (0.05) | 0.30 | (0.14) | 0.60 | (0.44) |
| FeO | 30.8 | (2.5) | 43.7 | (1.8) | 38.2 | (2.5) | 42.2 | (2.3) | 42.1 | (4.5) | 36.0 | (1.0) |
| MnO | 0.20 | (0.04) | 0.28 | (0.04) | 0.26 | (0.03) | 0.26 | (0.04) | 0.26 | (0.07) | 0.22 | (0.03) |
| NiO | 1.24 | (0.32) | 1.38 | (0.39) | 1.37 | (0.27) | 1.93 | (0.45) | 1.48 | (0.68) | 2.90 | (0.50) |
| MgO | 16.6 | (1.2) | 15.2 | (1.2) | 17.2 | (0.9) | 17.0 | (1.1) | 17.9 | (2.9) | 19.9 | (0.9) |
| CaO | 1.12 | (0.93) | 0.47 | (0.71) | 0.87 | (1.01) | 0.96 | (0.93) | 0.29 | (0.26) | 2.19 | (0.36) |
| $Na_2O$ | 0.30 | (0.18) | 0.21 | (0.08) | 0.25 | (0.13) | 0.20 | (0.05) | 0.31 | (0.24) | 0.32 | (0.06) |
| $K_2O$ | 0.06 | (0.03) | 0.03 | (0.02) | 0.03 | (0.02) | 0.04 | (0.03) | 0.04 | (0.04) | 0.05 | (0.01) |
| $P_2O_5$ | 0.21 | (0.08) | 0.18 | (0.03) | 0.23 | (0.12) | 0.29 | (0.14) | 0.26 | (0.15) | 0.28 | (0.03) |
| S | 1.60 | (0.41) | 2.67 | (1.22) | 1.12 | (0.26) | 1.89 | (0.63) | 1.17 | (0.37) | 3.44 | (0.68) |
| Total | 80.9 | | 91.9 | | 89.2 | | 95.6 | | 95.0 | | 97.7 | |
| FM ratio | 50.9 | | 61.8 | | 55.5 | | 58.2 | | 57.0 | | 50.4 | |

*Obtained by using a 10 $\mu$m diameter beam; excluding mineral fragments that are >5 $\mu$m in diameter. All other analyses were obtained by using a 50 $\mu$m diameter beam.

Abbeviations: *N* = number of analyses; s.d. = standard deviations; FM ratio = Fe/(Fe + Mg) × 100 atomic ratio.

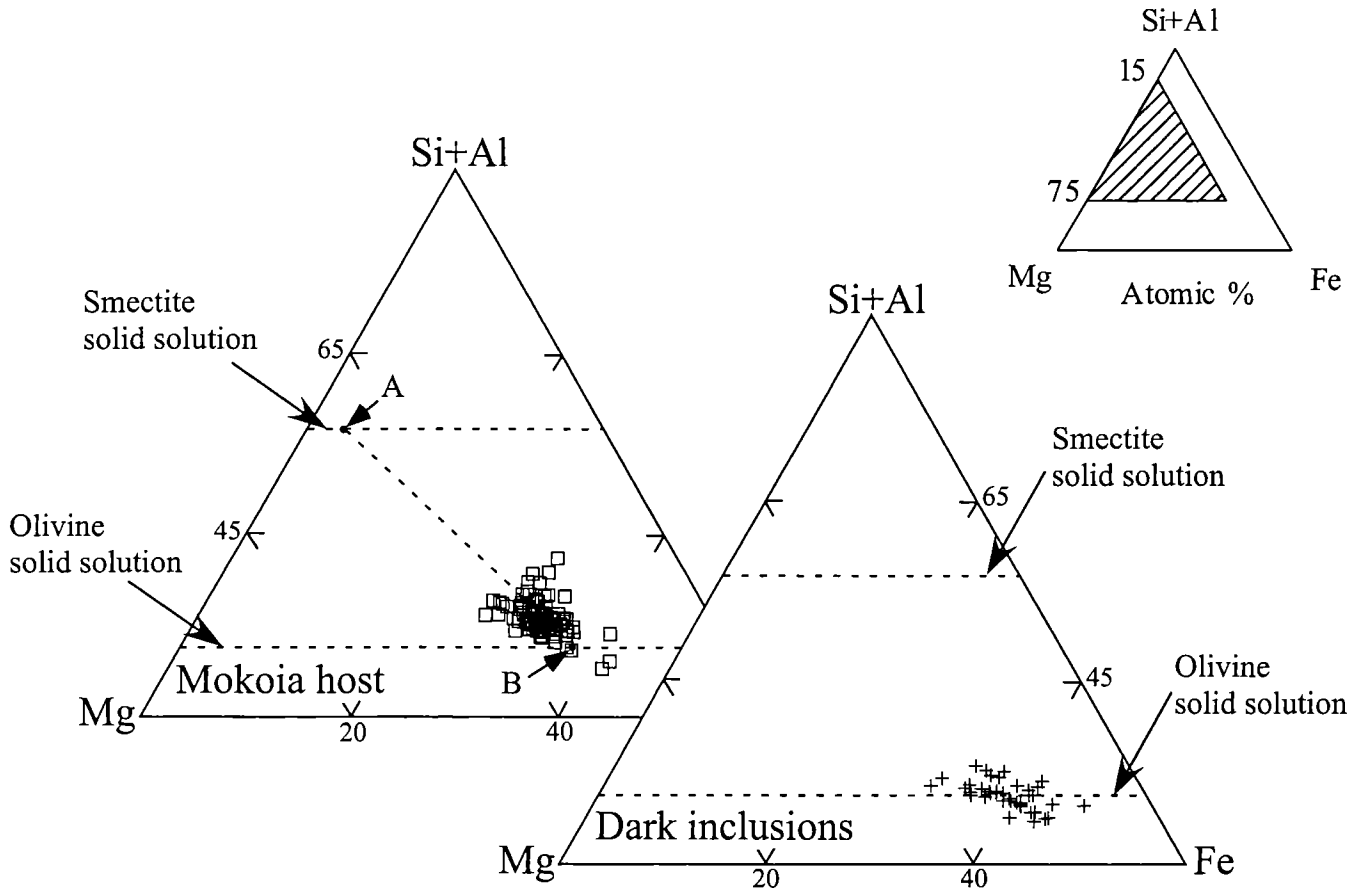


FIG. 9. Defocused-beam (50 $\mu$m in diameter) analyses of matrices of the dark inclusions and Mokoia host plotted in terms of atomic percents of Si + Al, Mg and Fe. Also shown are the ideal Mg-Fe solid solution lines of trioctahedral smectite ($(Mg, Fe)_3(Si, Al)_4O_{10}(OH)_2$) and olivine ($(Mg, Fe)_2SiO_4$). Indicated by A and B are the points at Fe/(Fe + Mg) = 0.07 on the smectite solid-solution line and at Fe/(Fe + Mg) = 0.54 on the olivine solid-solution line, respectively.

meteorite was probably removed. From these observations, we identify this material to be part of a melt vein. Defocused-beam WDS analyses and x-ray chemical mapping show that the matrix of this melt vein is similar in composition to the matrix of DI-3, but is significantly more enriched in Ca and S (Table 3; Fig. 11).

## DISCUSSION

### Relationship to the Host Meteorite

Our study has revealed that DIs occur abundantly in Mokoia and most of the DIs that we studied contain chondrules and chondrule fragments in fine-grained matrices. Those chondrules and chondrule fragments have been replaced by phyllosilicates to minor extents similar to that in the host meteorite, and no porous aggregates of Fe-rich olivine that are common in Allende DIs are contained. From these characteristics, the Mokoia DIs can be classified as the chondrule-bearing type (Fruland *et al.*, 1978; Johnson *et al.*, 1990), which is type A in the classification of Krot *et al.* (1995). Based on the parent-body model for the origin of DIs (Kojima and Tomeoka, 1996; Krot *et al.*, 1997), the DIs in Mokoia are regarded to be clasts of a chondritic rock that has experienced only a minor degree of replacement process. The next key questions to be answered are how the DIs are related to their host meteorite and whether the DIs came from the Mokoia parent body or some other parent body.

A genetic relationship between DIs and their host CV3 chondrites has been commonly suggested, but no case has been presented that clearly indicates the relationship. It is obvious, however, that the Mokoia DIs and their host meteorite are closely related to each other in mineral constituents, texture and bulk chemical composition. Especially the fact that both the DIs and their host meteorite contain the same phyllosilicates (Fe-bearing saponite and Na-rich phlogopite) in the same locations in chondrules and matrix provides decisive evidence that the DIs and their host meteorite have constituted a common parent body. The fact also indicates that the DIs have experienced aqueous alteration in conditions similar to those for the host meteorite in their parent body.

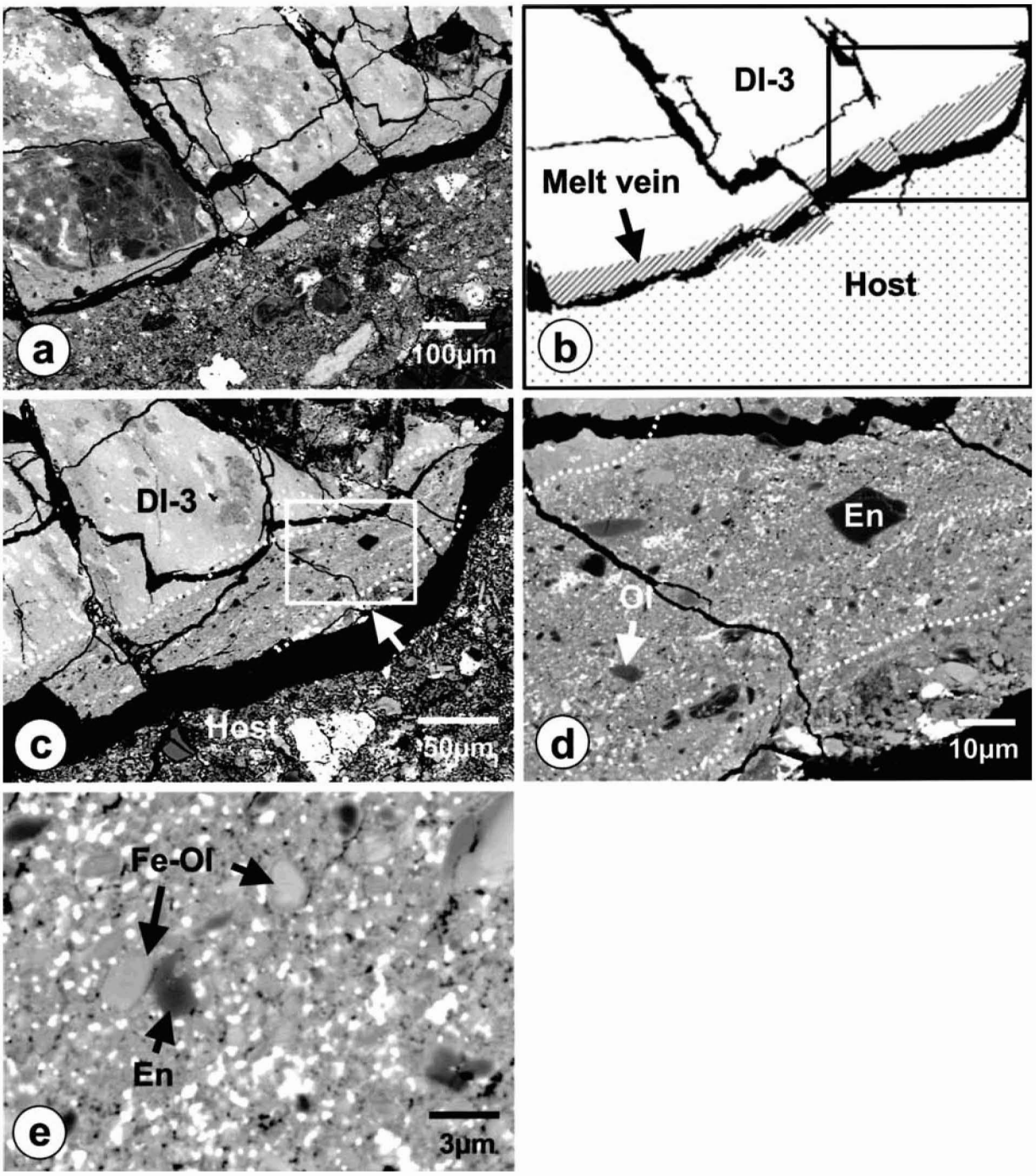


FIG. 10. (a) Backscattered electron image of a melt vein in DI-3. The vein is located along an edge of the DI. (b) Illustration of the image in (a). (c) Image of boxed area in (b), showing a portion of the melt vein. Note that a small lenticular area (indicated by a white arrow) having the same lithology as the DI matrix is attached to the vein. (d) Image of boxed area in (c), showing that the melt vein contains fragments of olivine (Ol) and enstatite (En). (e) High-magnification image of a portion of the melt vein, showing that the vein contains numerous rounded inclusions of pentlandite and magnetite (bright particles) and rounded pores as well as fragments of Fe-rich olivine (Fe-Ol) and enstatite.

Despite these indications of genetic relationship, our study has also revealed that the DIs have major characteristics that differ distinctly from the host meteorite as follows:

(1) Olivine grains in the matrices of the DIs are more homogeneous in Fe/(Fe + Mg) ratio than those in the host meteorite.

(2) Weight percent analytical totals of phyllosilicates in the DIs are consistently higher than those in the host meteorite, and higher than those of normal phyllosilicates.

(3) The matrices in the DIs are more compacted than those in the host meteorite.

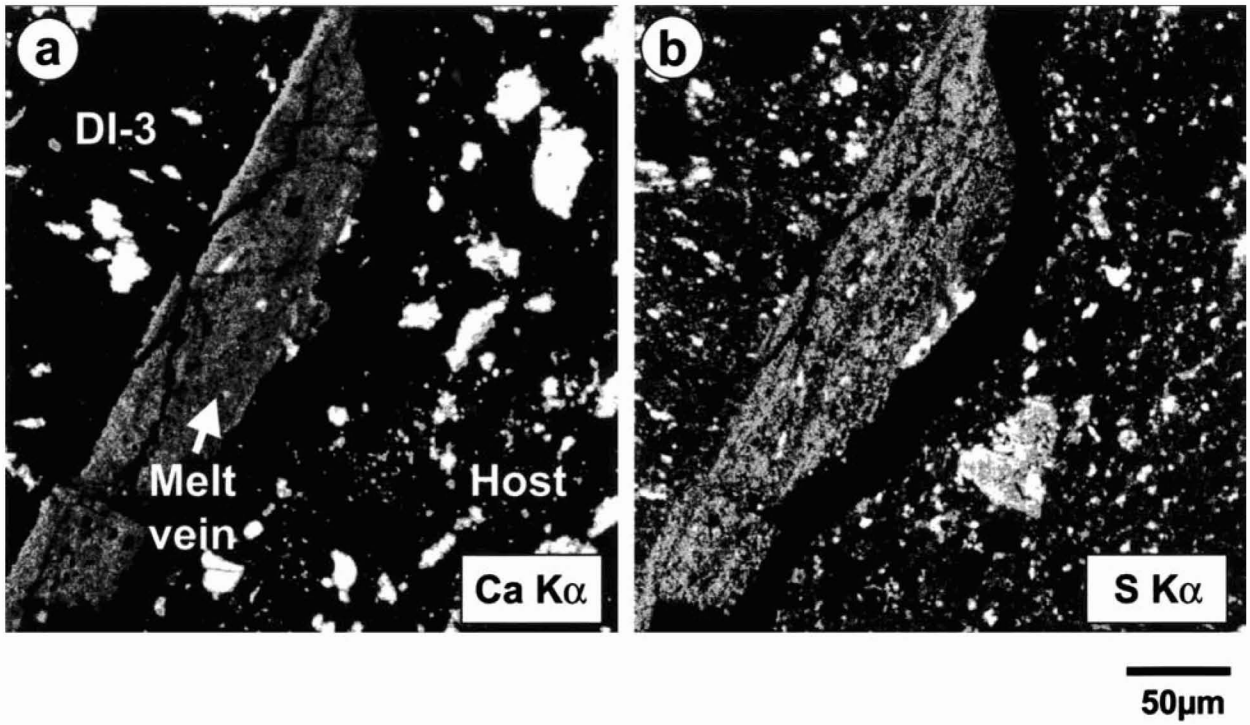


FIG. 11. X-ray chemical maps of Ca Kα (a) and S Kα (b) of a melt vein in DI-3. The maps (in which the brighter an area is, the higher the concentration of an element is) indicate that Ca and S are distinctly enriched in the melt vein matrix relative to both the DI matrix and the host meteorite matrix.

(4) Phyllosilicates in the matrices of the DIs are less abundant than in the matrix of the host meteorite.

All these characteristics were probably caused by secondary processes that had been experienced by the DIs before their incorporation into the host meteorite. In the following we will discuss the nature of the secondary processes that caused each of these characteristics.

**Evidence for Thermal Metamorphism and Dehydration**

Characteristic (1) suggests that the DIs have gone through thermal metamorphism in the meteorite parent body. Thermal metamorphism equilibrates the Fe/(Fe + Mg) distribution of olivines in fine-grained meteorite matrix due to solid-state diffusive exchange between Fe-poor olivines and Fe-rich olivines. At the initiation of thermal metamorphism, Fe also diffuses out from Fe-rich minerals such as magnetite and Fe-Ni sulfide in matrix, resulting in Fe enrichment of olivines in matrix. These processes clearly occurred in all the DIs in Mokoia. However, olivine grains in the DI matrices show relatively broad peaks in Fe/(Fe + Mg) distribution (Fig. 6). Chondrules contain coarse-grained phenocrysts of almost Fe-free olivine without any significant Fe-Mg zoning, and some chondrules contain Na-Ca-Al-rich glassy material in their mesostases. These characteristics indicate that although thermal metamorphism occurred, it was not so intense and did not go to completion.

Characteristic (2) suggests that phyllosilicates have been partially dehydrated by heating, and so serves as another indicator of thermal metamorphism. Saponite starts to decompose to pyroxene and silica at ~800 °C (Weiss *et al.*, 1955; MacKenzie, 1970; Akai, 1992). So the temperature probably exceeded this degree, which is well in the range for metamorphic temperatures of petrologic type 5–6. However, analytical totals of saponite, which are related to the degree of dehydration, are well below 100 wt% and differ considerably among DIs 1–4. These suggest incomplete dehydration and heterogeneous temperature distribution, and are consistent with the incomplete equilibration of matrix olivines in the DIs. From these results, it is probable that although the temperature exceeded 800 °C, the duration of heating was very short, and thermal metamorphism ceased at its initiation.

Despite the apparent indication of dehydration, most phyllosilicates in the DIs show fluffy, rugged appearance (Fig. 2d) identical to those in the host meteorite. This suggests that the phyllosilicates were transformed to anhydrous silicates without changing original morphology. Phyllosilicates that are completely dehydrated to olivine but show original fibrous texture have been frequently observed in thermally dehydrated CI and CM chondrites (Akai, 1988, 1990, 1992; Tomeoka *et al.*, 1989a,b; Tomeoka, 1990). DIs in Allende and other CV3 chondrites commonly contain fine grains of olivine having swirly fibrous morphology (*e.g.*, see Kojima and Tomeoka, 1996). Our observations support the interpretation that those

olivine grains in CV3 DIs have been formed by dehydration of phyllosilicates (Kojima *et al.*, 1993; Kojima and Tomeoka, 1996).

These results are consistent with the contention previously proposed for the DIs in other CV3 chondrites (*e.g.*, Vigarano, Allende, Efremovka) (Kojima *et al.*, 1993; Kojima and Tomeoka, 1996; Krot *et al.*, 1997, 1998a, 1999), that is, the DIs have experienced aqueous alteration and subsequent dehydration on the CV (or CV-like) parent body.

**Effects of Shock Metamorphism**

Characteristic (3) suggests that the DIs in Mokoia have experienced additional metamorphism due to shock. Most previously reported DIs appear not to have experienced significant shock metamorphism (Fruland *et al.*, 1978; Johnson *et al.*, 1990; Krot *et al.*, 1997). The compacted matrices of DIs in Mokoia closely resemble those in the Leoville, Efremovka, Bali and Grosnaja CV3 chondrites (Nakamura *et al.*, 1992, 2000; Krot *et al.*, 1995, 1998a) that are relatively highly shocked (to shock stage S3–S4) among the CV3 chondrites (Scott *et al.*, 1992). Especially DI-3 and DI-4 show very low porosities (0.2–2.1%) that are comparable to those of the matrices of Efremovka (1%) and Bali (2%) (Corrigan *et al.*, 1997; porosities for Leoville and Grosnaja are not available). The abundant occurrence of planar fractures in olivines and the presence of foliation in the matrices in DI-3 and DI-4 are also common with the highly shocked CV3 chondrites. Taking these into account, characteristic (4) of the Mokoia DIs can be explained by that phyllosilicates, which have a fluffy, fibrous nature, in interstices between fine olivine grains were squeezed due to shock compression and partially dehydrated due to shock heating, thus they diminished.

From these observations and evidence, the melt veins that occur in DI-3 and another small DI are probably of shock-induced origin. Silicate-rich local melts are extremely rare in type 1–3 carbonaceous chondrites, but have been reported from Efremovka that is assigned to the highest shock stage (S4) of the CV3 group (Scott *et al.*, 1992). Recently Tomeoka *et al.* (1999) conducted shock experiments of the Murchison CM chondrite and showed that local melting, such as melt veins and pockets, occurs at peak pressures from 20 to 30 GPa. Shock experiments of the Allende CV3 chondrite by Kiriyama *et al.* (2000) showed that similar local melting occurs at pressures from 25 to 35 GPa. The melts produced in both Murchison and Allende contain numerous globules of Fe-Ni sulfide and vesicles as well as small fragments of olivine and pyroxene. Those local melts were produced from the meteorite matrices but are enriched in Fe and S and sometimes in Ca relative to the matrices. These textural and compositional characteristics resemble those in the melt veins in the Mokoia DIs. From these results, it is probable that DI-3, another small DI containing a melt vein, and perhaps DI-4 have experienced shock compression equivalent to an experimental shock at peak pressures of 25–35 GPa.

Another important question that should be addressed is whether the thermal metamorphism and the shock metamorphism of the Mokoia DIs are related to each other. The probable short duration of heating and the heterogeneous temperature distribution in the DIs suggest that the thermal metamorphism is most likely to have been driven by shock heating. As already mentioned, the intensity of shock compression increases in the order of (1) Mokoia host, (2) DI-1 and DI-2, and (3) DI-3 and DI-4. On the other hand, phyllosilicates in DI-3 and DI-4 have a tendency to have higher analytical totals than those in DI-1 and DI-2 (see Table 2), which suggests that the former were more dehydrated (thus more heated) than the latter. So the degree of heating appears to increase in the order of (1) Mokoia host, (2) DI-1 and DI-2, and (3) DI-3 and DI-4, which is the same as for the increasing degree of shock compression. From these results, we suggest that a substantial portion of heat responsible for the thermal metamorphism in the DIs was generated by impacts, although we are uncertain whether it is a unique source of heat in the parent body.

**Comparison with Other CV3 Chondrites and Dark Inclusions**

Weisberg *et al.* (1997) proposed that oxidized CV3 chondrites, which include Mokoia, can be divided into two major lithologies, Bali-like and Allende-like, in which chondrules, CAIs and matrix show characteristic alteration features. Krot *et al.* (1998a,b) described detailed mineralogies of those two types of lithologies. We here compare the Mokoia DIs to those two types of lithologies. The Bali-like lithology is characterized by the presence of phyllosilicates, and it appears to have formed at relatively low temperatures (<300 °C) in the presence of aqueous solutions. The Allende-like lithology contains a variety of secondary minerals similar to the Bali-like lithology, but lacks phyllosilicates, so it appears to have experienced thermal dehydration after aqueous alteration. Krot *et al.* (1998a) regarded that Allende DIs are Allende-like and Mokoia host are Bali-like. However, our study reveals that the Mokoia DIs are Bali-like, and Bali, as wells as Grosnaja, is actually more similar to the DIs than Mokoia host in that it is highly shocked (to shock stage S3) and contains minor amounts of phyllosilicates. The similarity suggests that Bali and Grosnaja have gone through, like the DIs in Mokoia, thermal and shock metamorphism after aqueous alteration but have not been dehydrated to completion. So it appears that there are considerable metamorphic variations among the meteorites within the Bali-like group. Mokoia host probably represents the least metamorphosed lithology among the meteorites in the Bali-like group.

**Mokoia Parent Body Implied by Dark Inclusions**

It has been widely regarded that type-3 chondrites have experienced only minor aqueous alteration and thermal

metamorphism; therefore, they preserve the most primitive materials established in the solar nebula (*e.g.*, McSween, 1979). However, a number of previous studies have revealed that CV3 chondrites have experienced various kinds of replacement reactions including phyllosilicate formation from anhydrous silicates, ferrous olivine formation from forsterite, and alkali-halogen metasomatism in chondrules and CAIs (*e.g.*, Tomeoka and Buseck, 1982a,b, 1990; Keller and Buseck, 1990; Weinbruch *et al.*, 1990; Keller *et al.*, 1994; Hua and Buseck, 1995, 1998; Ikeda and Kimura, 1995; Kimura and Ikeda, 1995, 1998; Lee *et al.*, 1996; Brearley, 1997; Krot *et al.*, 1995, 1997, 1998a; Tomeoka and Tanimura, 2000), although whether the reactions occurred before or after accretion to the parent body has been controversial. Especially recent studies of DIs in CV3 chondrites suggested that aqueous alteration and thermal dehydration occurred extensively in the CV parent body.

Our study provides new insight into the processes that presumably occurred in the Mokoia parent body. It is particularly important that our study has revealed that the Mokoia DIs and their host meteorite have constituted a common parent body. This indicates that the Mokoia parent body was *not* such a body that is homogeneous throughout and has suffered no significant thermal and shock metamorphism. Rather the parent body was a heterogeneous conglomerate of rocks, each of which has suffered different degree of thermal and shock metamorphism. It is rather surprising that the degree of shock and thermal metamorphism ranges from almost none, as represented by the host meteorite, to those shocked to shock stage S4 and heated to such high temperatures to produce local melts, as represented by the DIs. This implies that the events that caused thermal and shock metamorphism occurred locally on the surface of the parent body.

We propose the following model for the Mokoia parent body. We presume that the parent body originally consisted of a heterogeneous mixture of ice and anhydrous rock. As the parent body acquired a heat source, aqueous alteration proceeded pervasively, so the lithology now seen in the host meteorite was produced. We are uncertain whether the heat at this initial stage was derived from impacts or some other source such as decay of radionuclide. From the limited extent of hydration in Mokoia, the aqueous alteration probably occurred in the presence of small amounts of solutions. Subsequently impact events occurred locally on the surface of the parent body, resulting in various extents of shock and thermal metamorphism. Consequently, the degree of shock and thermal metamorphism varied widely from location to location on the surface. Simultaneously brecciation proceeded and intermixed rocks from various locations in the parent body. The host Mokoia meteorite perhaps represents a region that escaped such impacts, while DIs came from a region or regions that suffered relatively strong impacts.

*Acknowledgments*–We thank Dr. J. A. Wood for providing the Mokoia samples, Drs. X. Hua and A. Krot for helpful reviews. Electron microprobe analysis was performed at the Venture Business Laboratory, Kobe University. This work was supported by Grant-in-Aid of the Japan Ministry of Educations, Science and Culture (No. 12440149).

*Editorial handling*: E. R. D. Scott

## REFERENCES

AKAI J. (1988) Incompletely transformed serpentine-type phyllosilicates in the matrix of Antarctic CM chondrites. *Geochim. Cosmochim. Acta* **52**, 1593–1599.

AKAI J. (1990) Mineralogical evidence of heating events in Antarctic carbonaceous chondrites, Y-86720 and Y-82162. *Proc. NIPR Symp. Antarct. Meteorites* **3**, 55–68.

AKAI J. (1992) T–T–T diagram of serpentine and saponite, and estimation of metamorphic heating degree of Antarctic carbonaceous chondrites. *Proc. NIPR Symp. Antarct. Meteorites* **5**, 120–135.

BREARLEY A. J. (1997) Disordered biopyriboles, amphibole, and talc in the Allende meteorite: Products of nebular or parent body aqueous alteration? *Science* **276**, 1103–1105.

BUCHANAN P. C., ZOLENSKY M. E. AND REID A. M. (1997) Petrology of Allende dark inclusions. *Geochim. Cosmochim. Acta* **61**, 1733–1743.

BUNCH T. E., CHANG S. AND OTT U. (1980) Regolith origin for Allende meteorite (abstract). *Lunar Planet. Sci.* **11**, 119–121.

COHEN R. E., KORNACKI A. S. AND WOOD J. A. (1983) Mineralogy and petrology of chondrules and inclusions in the Mokoia CV3 chondrite. *Geochim. Cosmochim. Acta* **47**, 1739–1757.

CORRIGAN C. M., ZOLENSKY M. E., DAHL J., LONG M., WEIR J., SAPP C. AND BURKETT P. J. (1997) The porosity and permeability of chondritic meteorites and interplanetary dust particles. *Meteorit. Planet. Sci.* **32**, 509–515.

FRULAND R. M., KING E. A. AND MCKAY D. S. (1978) Allende dark inclusions. *Proc. Lunar Planet. Sci. Conf.* **9th**, 1305–1329.

HUA X. AND BUSECK P. R. (1995) Fayalite in the Kaba and Mokoia carbonaceous chondrites. *Geochim. Cosmochim. Acta* **59**, 563–578.

HUA X. AND BUSECK P. R. (1998) Fayalitic halos around inclusions in forsterites from carbonaceous chondrites. *Geochim. Cosmochim. Acta* **62**, 1443–1458.

IKEDA Y. AND KIMURA M. (1995) Anhydrous alteration of Allende chondrules in the solar nebula I: Description and alteration of chondrules with known oxygen-isotopic compositions. *Proc. NIPR Symp. Antarct. Meteorites* **8**, 97–122.

ITOH D. AND TOMEOKA K. (2002) Dark inclusions in CO3 chondrites: New indicators of parent-body processes. *Geochim. Cosmochim. Acta* **66** (in press).

JOHNSON C. A., PRINZ M., WEISBERG M. K., CLAYTON R. N. AND MAYEDA T. K. (1990) Dark inclusions in Allende, Leoville, and Vigarano: Evidence for nebular oxidation of CV3 constituents. *Geochim. Cosmochim. Acta* **54**, 819–830.

KELLER L. P. AND BUSECK P. R. (1990) Aqueous alteration in the Kaba CV3 carbonaceous chondrite. *Geochim. Cosmochim. Acta* **54**, 2113–2120.

KELLER L. P., THOMAS K. L., CLAYTON R. N., MAYEDA T. K., DEHART J. M. AND MCKAY D. S. (1994) Aqueous alteration of the Bali CV3 chondrite: Evidence from mineralogy, mineral chemistry, and oxygen isotopic compositions. *Geochim. Cosmochim. Acta* **58**, 5589–5598.

KIMURA M. AND IKEDA Y. (1995) Anhydrous alteration of Allende chondrules in the solar nebula II: Alkali-Ca exchange reactions and formation of nepheline, sodalite and Ca-rich phases in chondrules. *Proc. NIPR Symp. Antarct. Meteorites* **8**, 123–138.

KIMURA M. AND IKEDA Y. (1998) Hydrous and anhydrous alterations of chondrules in Kaba and Mokoia CV chondrites. *Meteorit. Planet. Sci.* **33**, 1139–1146.

KIRIYAMA K., TOMEOKA K. AND SEKINE T. (2000) Experimental shock metamorphism of the Allende CV chondrite at pressures from 20 to 50 GPa (abstract). *Meteorit. Planet. Sci.* **35 (Suppl.)**, A88.

KOJIMA T. AND TOMEOKA K. (1996) Indicators of aqueous alteration and thermal metamorphism on the CV parent body: Microtextures of a dark inclusion from Allende. *Geochim. Cosmochim. Acta* **60**, 2651–2666.

KOJIMA T., TOMEOKA K. AND TAKEDA H. (1993) Unusual dark clasts in the Vigarano CV3 carbonaceous chondrite: Record of parent body process. *Meteoritics* **28**, 649–658.

KROT A. N., SCOTT E. R. D. AND ZOLENSKY M. E. (1995) Mineralogical and chemical modification of components in CV3 chondrites: Nebular or asteroidal processing? *Meteoritics* **30**, 748–775.

KROT A. N., SCOTT E. R. D. AND ZOLENSKY M. E. (1997) Origin of fayalitic olivine rims and lath-shaped matrix olivine in the CV3 chondrite Allende and its dark inclusions. *Meteorit. Planet. Sci.* **32**, 31–49.

KROT A. N., PETAEV M. I., ZOLENSKY M. E., KEIL K., SCOTT E. R. D. AND NAKAMURA K. (1998a) Secondary calcium-iron-rich minerals in the Bali-like and Allende-like oxidized CV3 chondrites and Allende dark inclusions. *Meteorit. Planet. Sci.* **33**, 623–645.

KROT A. N., PETAEV M. I., SCOTT E. R. D., CHOI B-G., ZOLENSKY M. E. AND KEIL K. (1998b) Progressive alteration in CV3 chondrites: More evidence for asteroidal alteration. *Meteorit. Planet. Sci.* **33**, 1065–1085.

KROT A. N., BREARLEY A. J., ULYANOV A. A., BIRYUKOV V. V., SWINDLE T. D., KEIL K., MITTLEFEHLDT D. W., SCOTT E. R. D., CLAYTON R. N. AND MAYEDA T. K. (1999) Mineralogy, petrography, bulk chemical, iodine-xenon, and oxygen-isotopic compositions of dark inclusions in the reduced CV3 chondrite Efremovka. *Meteorit. Planet. Sci.* **34**, 67–89.

KURAT G., PALME H., BRANDSTÄTTER F. AND HUTH J. (1989) Allende xenolith AF: Undisturbed record of condensation and aggregation of matter in the solar nebula. *Z. Naturforsch.* **44a**, 988–1004.

LEE M. R., HUTCHISON R. AND GRAHAM A. L. (1996) Aqueous alteration in the matrix of the Vigarano (CV3) carbonaceous chondrite. *Meteorit. Planet. Sci.* **31**, 477–483.

MACKENZIE R. C. (1970) Simple phyllosilicates based on gibbsite- and brucite-like sheets. In *Differential Thermal Analysis*, Vol. 1 (ed. R. C. MacKenzie), pp. 497–537. Academic Press, London, U.K.

MCSWEEN H. Y., JR. (1979) Are carbonaceous chondrites primitive or processed? A review. *Rev. Geophys. Space Phys.* **17**, 1059–1078.

NAKAMURA T., TOMEOKA K. AND TAKEDA H. (1992) Shock effects of the Leoville CV carbonaceous chondrite: A transmission electron microscope study. *Earth Planet. Sci. Lett.* **114**, 159–170.

NAKAMURA T., TOMEOKA K., TAKAOKA N., SEKINE T. AND TAKEDA H. (2000) Impact-induced textural changes of CV carbonaceous chondrites: Experimental reproduction. *Icarus* **146**, 289–300.

PALME H., KURAT G., SPETTEL B. AND BURGHELE A. (1989) Chemical composition of an unusual xenolith of the Allende meteorite. *Z. Naturforsch.* **44a**, 1005–1014.

SCOTT E. R. D., BARBER D. J., ALEXANDER C. M., HUTCHISON R. AND PECK J. A. (1988) Primitive material surviving in chondrites: Matrix. In *Meteorites and the Early Solar System* (eds. J. F. Kerridge and M. S. Matthews), pp. 718–745. Univ. Arizona Press, Tucson, Arizona, USA.

SCOTT E. R. D., KEIL K. AND STÖFFLER D. (1992) Shock metamorphism of carbonaceous chondrites. *Geochim. Cosmochim. Acta* **56**, 4281–4293.

TOMEOKA K. (1990) Mineralogy and petrology of Belgica-7904: A new kind of carbonaceous chondrite from Antarctica. *Proc. NIPR Symp. Antarct. Meteorites* **3**, 40–54.

TOMEOKA K. AND BUSECK P. R. (1982a) Intergrown mica and montmorillonite in the Allende carbonaceous chondrite. *Nature* **299**, 326–327.

TOMEOKA K. AND BUSECK P. R. (1982b) An unusual layered mineral in chondrules and aggregates of the Allende carbonaceous chondrite. *Nature* **299**, 327–329.

TOMEOKA K. AND BUSECK P. R. (1990) Phyllosilicates in the Mokoia CV carbonaceous chondrite: Evidence for aqueous alteration in an oxidizing environment. *Geochim. Cosmochim. Acta* **54**, 1745–1754.

TOMEOKA K. AND TANIMURA I. (2000) Phyllosilicate-rich chondrule rims in the Vigarano CV3 chondrite: Evidence for parent-body processes. *Geochim. Cosmochim. Acta* **64**, 1971–1988.

TOMEOKA K., KOJIMA H. AND YANAI K. (1989a) Yamato-82162: A new kind of CI carbonaceous chondrite found in Antarctica. *Proc. NIPR Symp. Antarct. Meteorites* **2**, 36–54.

TOMEOKA K., KOJIMA H. AND YANAI K. (1989b) Yamato-86720: A CM carbonaceous chondrite having experienced extensive aqueous alteration and thermal metamorphism. *Proc. NIPR Symp. Antarct. Meteorites* **2**, 55–74.

TOMEOKA K., YAMAHANA Y. AND SEKINE T. (1999) Experimental shock metamorphism of the Murchison CM carbonaceous chondrite. *Geochim. Cosmochim Acta* **63**, 3683–3703.

WEINBRUCH S., PALME H., MÜLLER W. F. AND EL GORESY A. (1990) FeO-rich rims and veins in Allende forsterite: Evidence for high temperature condensation at oxidizing conditions. *Meteoritics* **25**, 115–125.

WEISBERG M. K. AND PRINZ M. (1998) Fayalitic olivine in CV3 chondrite matrix and dark inclusions: A nebular origin. *Meteorit. Planet. Sci.* **33**, 1087–1099.

WEISBERG M. K., PRINZ M., CLAYTON R. N. AND MAYEDA T. K. (1997) CV3 chondrites: Three subgroups, not two (abstract). *Meteorit. Planet. Sci.* **32 (Suppl.)**, A138–A139.

WEISS A., KOCH G. AND HOFMANN U. (1955) Zur Kenntnis von Saponit. *Ber. Deut. Keram. Ges.* **32**, 12–17.